

Two Component Baryonic-Dark Matter Structure Formation in Top-Hat Model

M. Malekjani

*Department of Theoretical Physics and Astrophysics, University of Tabriz,
P.O.Box 51664, Tabriz, Iran
malekjani@tabrizu.ac.ir*

S. Rahvar

*Department of Physics, Sharif University of Technology, P.O.Box 11365-9161,
Tehran, Iran
rahvar@sharif.edu*

D. M. Z. Jassur

*Department of Theoretical Physics and Astrophysics, University of Tabriz,
P.O.Box 51664, Tabriz, Iran
jassur@tabrizu.ac.ir*

Abstract

In this work we extend simple top-hat model of structure formation to the two-component system made of baryonic and dark matter. We use Harrison-Zeldovich spectrum as the initial condition for the structures and calculate their evolution up to the present time. While we do not take into account some complications during the structure formation, such as the merging of galaxies, however this formalism can give us a qualitative picture from the formation of structures. We show that in this model small scale structures evolve faster than the larger ones and it predicts a down-top scenario for the structure formation. The trend of power spectrum in this model is compatible with the observations and results in $\sigma_8 \sim 0.8$. This formalism provides an analytic treatment of structure growth and can easily show the effect of the cosmological parameters on the formation of the structures. As an example, the effect of a parameterized dark energy model on the growth of the structures is investigated.

Key words: cosmology, large scale structure formation, galaxy formation

1 Introduction

Observations of the Cosmic Microwave Background (CMB) by the COBE satellite and the subsequent experiments such as WMAP indicate the existence of temperature fluctuations of order $\sim 10^{-5}$ at the last scattering surface (1; 2; 3). This temperature contrast on CMB may result from the primordial quantum fluctuations at the early universe. The quantum fluctuations in the inflationary scenario, provide a specific spectrum for the matter so-called Harrison-Zeldovich. However, Recent observations by WMAP show a small deviation from this spectrum ($n_s = 0.958 \pm 0.016$) (4). An outstanding characteristic of this spectrum is its scale-independent property, means that all the perturbations have some density contrast of about 10^{-5} at the entering time to the horizon (5). One of the questions in cosmology is that of how these small perturbations at $z_{dec} = 1100$ can grow to the present non-linear structures while we expect from the standard structure formation theory that they should evolve to a density contrast of $\delta \sim \delta_{dec} \times z_{dec} = 10^{-2}$ at the present time (6).

Including dark matter as one of the components of the universe is a solution to this question. Since the entering time of the structures to the horizon depends on the size of structure, we expect small scale structures enter earlier than the larger ones. Meanwhile, before the decoupling epoch, pressure of the radiation prevents formation of baryonic structures smaller than the Silk mass (7), the dark matter structures continue their growth. After decoupling, the mutual interaction of dark matter-baryonic matter speeds up the growing rate of the structure formation and results in non-linear structures at the present time.

Here in this work we use two components of baryonic and dark matter in the top-hat model for studying their growth. We take the initial condition of sub-horizon over-dense regions at the last scattering surface. The size of perturbations in our concern guarantees using of Newtonian mechanics (8; 9). After decoupling, the top-hat sphere starts to expand up to a maximum radius and then turns-around to collapse. During the collapse, once the structure satisfies the virial condition, the global velocity turns into the dispersion velocity and thermalizes the gas of structure and finally prevents a catastrophic collapse of the structure. The result of thermalization is the ionization of the baryonic gas and consequently gas starts to cool through the radiation. Cooling makes baryonic structure to contract further and finally the baryonic component reaches to a stable stage. We should point out that in this scenario we ignore merging effects during the formation of the structures and this model can be applicable only for the isolated systems. Finally we compare σ_8 from this simple theoretical model with that from weak-lensing.

The organization of paper is as follows: In Section 2 we introduce Standard

Collapse Model (SCM), extend it for the two component fluid and obtain dynamics and power spectrum of the structures. Section 3 discusses about the effect of variable dark energy on the formation of structure in top-hat model. In Section 4 we study the cooling effect on the evolution of baryonic matter after the thermalization and estimate corresponding redshift for the star formation. We conclude in section 5.

2 Spherical Top-Hat Model: Structure Formation

In this section we review the standard spherical collapse model. Here we take a spatial uniform distribution of the matter inside the structure, so-called top-hat distribution which is slightly denser than the uniform background density. One of the advantages of this model is that it has an analytical solution for the dynamics of the structure. In this section first we introduce the standard top-hat model and then extend it, introducing the two component fluid in the structure: (i) a non-dissipative dark matter and (ii) a dissipative baryonic matter.

2.1 standard top-hat model

A simple approach for studying the structure formation in the universe is the spherical collapse model. We take a spherical region embedded in the uniform background which has a tiny density deviation from that of the background. The scale of this region is much smaller than horizon and the velocities are non-relativistic. These two conditions guarantee the application of the Newtonian gravity for studying the growth of the structures (8; 9).

For a spherical region with the radius $R(t)$ and uniformly distributed mass of M , containing non-relativistic matter, the density contrast is given by:

$$1 + \delta(t) = \frac{\rho(t)}{\rho_b(t)} = \frac{3M}{4\pi R^3(t)} \frac{1}{\rho_b(t)}, \quad (1)$$

where $\rho_b(t)$ is the homogenous background density of the universe. The energy and momentum equations for a non-dissipative spherical matter is given by:

$$E = \frac{1}{2} \dot{R}(t)^2 - \frac{GM}{R(t)}, \quad (2)$$

$$\ddot{R}(t) = -\frac{GM}{R(t)^2} \quad (3)$$

where E is energy per mass and can be calculated from the initial condition of the structure, (i.e. $E = E_i$). The initial radial velocity of the structure is taken by $v_i = H_i R_i + v_i^{(pec)}$, where H_i is the Hubble parameter of the background and R_i is the size of the structure at the initial time, $v_i^{(pec)}$ is the peculiar velocity of the structure and can be given by $v_i^{(pec)} = -H_i R_i \delta_i$ (6). Using the dependence of the peculiar velocity to the density contrast, the radial velocity of the structure at the initial time is:

$$v_i = H_i R_i (1 - \delta_i), \quad (4)$$

where δ_i depends on the size of the structure. Using equation (4), the Kinetic energy per unit mass of the structure is $K_i = K_i^{(b)}(1 - 2\delta_i)$ where $K_i^{(b)}$ is the Kinetic energy of background at a distance R_i from the center of coordinate¹. For the initial potential energy of structure we have $U_i = \Omega_i K_i^{(b)}(1 + \delta_i)$. The total energy is given by the sum of the kinetic and the potential energy of the structure at the initial time as:

$$E = -k_i^{(b)} \Omega_i (1 + \delta_i + 2\delta_i \Omega_i^{-1} - \Omega_i^{-1}). \quad (5)$$

For the case of spatially flat universe, $E = -3k_i^{(b)} \delta_i$. Integrating from equation (2) results in the equation of motion in the parametric form:

$$R(\theta) = A(1 - \cos \theta), \quad (6)$$

$$t(\theta) = T + B(\theta - \sin \theta), \quad (7)$$

where θ varies in the range of $\in [0, 2\pi]$ and T is a constant. For $\theta = \pi$, the structure reaches to the maximum radius of $r_{max} = 2A$. Substituting in equation (2) at the maximum radius provides $A = GM/2E$ which results in

$$A = \frac{1}{6} \frac{R_i}{\delta_i}$$

On the other hand using equation (3) yields:

$$A^3 = GMB^2$$

Substituting equations (6) and (7) in (1) results the evolution of the density contrast in terms of θ as:

$$\delta = \frac{9(\theta - \sin \theta)^2}{2(1 - \cos \theta)^3} - 1. \quad (8)$$

¹ Note that the effect of density contrast in the velocity of the structure and subsequently on the Kinetic Energy of over-dense region is missed in the text book (10).

For the initial condition, considering $\delta_i \ll 1$, the initial phase is $\theta_i = 2\sqrt{\delta_i}$. Taking $T = 0$, $t(\theta)$ will coincide with the cosmic time. From the initial condition, B obtain as:

$$B = \frac{3t_i}{4\delta_i^{3/2}}.$$

From equation (8) at $\theta = 2\pi/3$ the structure enters to the non-linear regime (i.e. $\delta \simeq 1$).

On the other hand for $\theta = 2\pi$ we have singularity, however before this stage, global radial velocity of the structure is converted to the dispersion velocity and prevent it from the catastrophic collapsing. The virial theorem provides us a radius that the stable condition of the structure is fulfilled. In the next part we will extend the top-hat model to the two component fluid of the baryonic and dark matter in which they are gravitationally coupled during the evolution of the structure.

2.2 two component top-hat model

Evolution of the large scale structures indicates that dark matter is an essential element for the formation of the structures in the universe. In the standard scenario of the structure formation, structures composed by baryonic matter and dark matter are in mutual gravitational interaction during their evolution. In this section we obtain the evolution of each component in the structure, using the top-hat model.

Let us start with baryonic component. Baryons before the decoupling were tightly coupled to the photons and diffusion of the radiation prevents them to collapse under their own gravity. The corresponding diffusive mass of the baryonic structure with $\lambda < l_{diff}$ is called the Silk mass with the mass of $M_S = 6.2 \times 10^{12} (\Omega/\Omega_B)^{3/2} (\Omega h^2)^{-3/4} M_\odot$ (11). However, after decoupling of the baryons from the cosmic microwave background radiation, Jeans length decreased rapidly and baryonic structure could grow freely (see Fig. 1). The corresponding Jeans mass after the decoupling is

$$M_J = \rho_b \left(\frac{kT}{G\rho_b m_p} \right)^{3/2} \simeq 10^5 M_\odot, \quad (9)$$

where all the parameters are calculated at the last scattering surface with $T \sim 3000K$ and m_p is the mass of the proton. The rest of the scenario is the gravitational interaction of the baryonic matter larger than the corresponding Jeans mass with the gravitational potentials that have already been made by the dark matter structures.

Comparing the mass of galaxies and cluster of galaxies with the Silk mass at the last scattering surface shows that we can set $\delta_b < 10^{-5}$ which can be ignored compare to the density contrast of dark matter ($\delta_b \ll \delta_d \simeq 10^{-3}$).

We consider two spherical regions with radii of $R_b(t)$ and $R_d(t)$, and total masses of M_b and M_d for the baryonic and dark matter components of the structure. These two spheres are coincided on each other at the initial time, but due to the different initial conditions they will evolve with different rates. Similar to the first part of this section, the momentum and energy conservation equations for the dark matter is written as

$$\ddot{R}_d = -G \frac{M_d + M_b(t)}{R_d^2}, \quad (10)$$

$$E_d = \frac{1}{2} \dot{R}_d^2 - G \frac{M_d + M_b(t)}{R_d}. \quad (11)$$

We let the initial density-contrast for the baryonic matter ($\delta_b \simeq 0$) which provides a zero initial peculiar velocity for the baryonic component. Comparing to the dark matter sphere, the baryonic sphere will expand faster. According to this picture from the dynamics, the dark matter will interact gravitationally only with a fraction of the baryonic matter inside the dark matter sphere.

Similarly, the dynamics of baryonic sphere is given by:

$$\ddot{R}_b = -G \frac{M_d + M_b}{R_b^2}, \quad (12)$$

$$E_b = \frac{1}{2} \dot{R}_b^2 - G \frac{M_d + M_b}{R_b}. \quad (13)$$

As the baryonic sphere is always larger than the dark matter sphere, this component interacts with all the dark sphere. The energy of the two spheres can be obtained from Eq.(5). Setting zero peculiar velocity for the baryonic sphere, results in $E_b = -k_i^{(b)} \delta_i^{(d)}$ and for the dark matter component $E_d = -3k_i^{(b)} \delta_i^{(d)}$.

To calculate the initial condition for the density contrast of dark matter $\delta_i^{(d)}$, we use the Harrison-Zeldovich power-law spectrum (12; 13) as

$$P(k) = Ak^n, \quad (14)$$

where we adapt $n = 1$. The corresponding mass variance of this spectrum is $\sigma^2 = \frac{A}{4\pi^2} k^4$. An important specification of this spectrum is that at the entering time of the structure to the horizon the density contrast has an invariant value of $\sigma_{enter} = 2\pi A^{1/2} / (9t_0^2)$. Using $A \simeq (28.6 h^{-1} \text{ Mpc})^4$, the density contrast for

the entering time is $\delta_{enter} \simeq 6 \times 10^{-5}$. Our aim at this stage is applying the Harrison-Zeldovich spectrum to have the density contrast of the dark matter at the decoupling time. The density contrast at the last scattering depends on the epoch that structure enters to the horizon. We divide the evolution of density contrast into two area of radiation and matter dominant epochs. In these two phases, the dynamics of dark matter changes with different rates in terms of scale factor.

Let us first consider the structures that enter the horizon at the radiation dominant epoch. The structures having smaller than the horizon mass at the equality time ($M < M_H(eq)$) will enter horizon at the following redshift:

$$z_{enter}(M) \simeq z_{eq} \left(\frac{M}{M_H(z_{eq})} \right)^{-\frac{1}{3}}. \quad (15)$$

Letting horizon mass at the equality epoch $M_H(z_{eq}) \simeq 5 \times 10^{15} (\Omega h^2)^{-2} M_\odot$, the corresponding entering redshift of a structure to the horizon can be calculated. For instance the dark matter component of a structure with a galaxy mass enters the horizon at $z_{enter}(galaxy) \sim 5.90 \times 10^4$. The structures grow during z_{enter} (enter time) to z_{eq} (equality time) by a logarithmic factor of

$$\delta(a_{eq}) \simeq 5 \ln \left(\frac{a_{eq}}{a_{enter}} \right) \delta(enter), \quad (16)$$

where we use $z_{eq} = 3454^{+385}_{-392}$ (3). Structure with a galaxy size at the present time will grow by the factor of 20 during z_{enter} to z_{eq} period which results a density contrast of about $\delta_{eq}(galaxy) \sim 8.50 \times 10^{-4}$ at equality time. Once the universe enters to the matter dominate era, structure start to grow proportional to the scale factor and at the decoupling time the density contrast of dark matter will reach to $\delta(z_{dec}) = a_{dec}/a_{enter} \times \delta_{enter}$. For a structure with the galaxy mass, the dark matter density contrast grows up to $\delta_{dec} \simeq 2.7 \times 10^{-3}$ at the decoupling time (we use $z_{dec} = 1088^{+1}_{-2}$ (3)). Fig.(2) shows the dynamics of the radii of dark matter and baryonic components of a galaxy in terms of redshift. We use Λ CDM model for the background with the parameters of $\Omega_m^{(0)} = 0.3$, $\Omega_\Lambda^{(0)} = 0.7$ and $H_0 \sim 70 \text{ Km/sMpc}^{-1}$. The time dependence of density contrast also is shown in Fig. (3). The evolution of each component is calculated up to the virilization time. We note that the dark matter component virialize earlier than the baryonic part.

We calculate the evolution of the gravitationally coupled two component in the top-hat model, for the structures in the range of 10^6 to 10^{15} solar masses. These structures, depending on their masses, will enter the horizon at different epochs, smaller sooner and the larger later. Means that the smaller structures grow faster than larger ones (see Table 1 and Fig. 4). This result is in agreement with the down-top scenario of the structure formation.

An important observational data for examining this model is comparing the power spectrum of the large scale structures at the present time with that of model. We do this comparison by calculating the mass variance for a sphere with the radius of R , in terms of power spectrum. The total mass $M_R(r)$ in a sphere with the radius R , centered on the point r is:

$$\begin{aligned} M_R(r) &= \int_{|r-r'| < R} \rho(r') d^3 r' \\ &= \int \rho(r') \Theta(R - |r - r'|) d^3 r', \end{aligned} \quad (17)$$

where Θ is the step function. Using the Fourier transformation of density contrast and step function, the mass variance is related to the power-spectrum through

$$\left(\frac{\Delta M_R}{M} \right)^2 = \int |W(kR)|^2 |\Delta_k|^2 \frac{dk}{k}, \quad (18)$$

where $\Delta_k = k^{3/2} |\delta_k| / \sqrt{2\pi}$ and $W(kR)$ is the Fourier transformation of step function. The function $W(kR)$ cuts off the integral (18) for $k > 1/R$ and since Δ_k is an increasing function of k , so the integral is generally dominated at $k \sim 1/R$ and we have (14):

$$\left(\frac{\Delta M_R}{M} \right) \sim \Delta_k \quad k \sim 1.38/R. \quad (19)$$

Figure (5) shows the calculated power spectrum in two component top-hat model in terms of k . This power spectrum derived from this model has almost the same trend as the observations (14). We should mention that since the power-spectrum of galaxies has scale dependent biasing, these data cannot be used for comparing with the dark matter spectrum. To have a comparison of this model with the observed data, we use σ_8 derived from the gravitational weak-lensing observations (15). We point out that σ_8 derived from the weak-lensing doesn't suffer from the biasing problem and it probes directly the distribution of the dark matter. Weak lensing observations provide $0.62 < \sigma_8 < 1.32$ which is compatible with that of top-hat model, $\sigma_8 \simeq 0.8$.

In the next section we will discuss about the effect of background dynamics on the evolution of the structures namely the effect of a variable dark energy model.

3 Top-Hat Model in Variable Dark Energy Background

In this section we discuss the effect of background dynamics on the growth rate of the structures. Recent observations of SNIa and CMB show that universe is mainly made by an exotic fluid so-called dark energy which speeds up its expansion (16). The standard solution for interpretation of the positive acceleration of the universe is including the cosmological constant to the Einstein equation. The best fit with the observations provides $\Omega_m^{(0)} = 0.3$ and $\Omega_\Lambda^{(0)} = 0.7$, where Ω_Λ is the density parameter corresponds to the cosmological constant. While Λ CDM model provides a good fit to the SNIa and CMB data, however it suffers the coincidence problem and finite tuning of the cosmological constant at the early universe. One of the solutions is considering a variable dark energy model. In this model an evolving scalar field generates the energy and the pressure of the dark energy and for the later times in the history of universe, it provides a positive accelerating universe.

In this section we study the effect of variable dark energy on the dynamics of the spherical collapse model as a function of the redshift. The dark energy can influence on the growth of large-scale cosmological structures through (i) the background effect, in which the dark energy changes the expansion rate of the background and (ii) dark energy may deviate from the homogenous distribution due to the gravitational interaction with the dark matter. The feedback of the dark energy is changing the growth rate of the dark matter. These effects have been studied in the following works (17; 18; 19; 20; 21; 22; 23).

In the case of Λ CDM universe the spherical collapse is similar to that in CDM model, except the cosmological constant that changes the growth of the structure though altering the background dynamics. For the CDM model the virialization radius (R_{vir}) is the half of the maximum radius of the structure (R_{max}). In the Λ CDM universe the virialization radius is smaller than that of in CDM model (17). Mota and Van de Bruck (MB) considered the spherical collapse for different potentials of the quintessence models (23). They showed that the predictions of the spherical collapse depend on the dark energy model. In this scenario, during the collapse of over-dense regions, the dark matter enters the highly non-linear regime while the perturbation in dark energy deviates slightly from the background. They also showed that if the dark energy equation of state is assumed to be constant, the differences between the homogenous and inhomogeneous cases are small. The advantage of considering the dark energy in the spherical collapse model is that it predicts that the cosmic structures such as the clusters of galaxy have been collapsed prior to the epoch of $z \sim 1.4$, compatible with the observations of the most distant cluster (29).

In this part we examine the effect of a parameterized dark energy on the evolution of the structures through the dynamics of the background. We take the equation of state from Wetterich (2004):

$$\omega(z; b, \omega_0) = \frac{\omega_0}{[1 + b \ln(1 + z)]^2}, \quad (20)$$

where ω_0 is the equation of state at the present time and b is the bending parameter (24). The best fit from the comparison of the cosmological data with the model results in $b = 1.35^{+1.65}_{-0.90}$ and $w_0 = -1.45^{+0.35}_{-0.60}$ (25). The density parameter of this dark energy from the continuity equation changes as:

$$\Omega_\lambda(z; b, \omega_0) = \Omega_\lambda^{(0)}(1 + z)^{3[1 + \bar{w}(z; b, \omega_0)]}, \quad (21)$$

where $\Omega_\lambda^{(0)}$ is the energy density of dark energy at the present time and $\bar{w}(z; b, \omega_0) = \omega_0/[1 + b \ln(1 + z)]$ is the average of the equation of state in the logarithmic scale. Using the Hubble parameter for the flat universe,

$$H^2(z; b, \omega_0) = H_0^2[\Omega_m^{(0)}(1 + z)^3 + \Omega_r^{(0)}(1 + z)^4 + \Omega_\lambda^{(0)}(1 + z)^{3(1 + \bar{w})}], \quad (22)$$

we obtain the dynamics of the scale factor for the various bending parameters as shown in Figure (6). To calculate the evolution of the baryonic and dark matter components of the structure, we use equations (10) and (12) to obtain the radius of the structure as a function of time. The evolution of the Hubble parameter as a function of redshift is given by equation (22). Eliminating time in favor of the redshift for the dynamics of the structures we obtain $R = R(z)$ as shown in Fig. (7). Here we fix the value of w_0 and calculate the dynamics of the structures for various bending parameters. Increasing the bending parameter causes the structure forms at earlier epochs but with smaller radius. Also the effect of w_0 on the formation of structures, while b is a fixed value, is shown in Fig. (8). Decreasing ω_0 causes the structures form faster with smaller radius.

In the dark energy models, the evolution of the structures deviate from that in Λ CDM model. This effect results from the change in the background dynamics due to the dark energy. In addition to this effect, the total energy of the structure will be changed due to the dark energy effect. The effect of a variable dark energy in contrast to Λ CDM model is that we can have a none-zero contribution of the dark energy at the early epoches of the universe. So for a given H_0 at the present time, we expect to have larger H_i at the early times. Looking to the total energy of a structure $E = -3/2 H_i^2 R_i^2 \delta_i$ shows that having larger H_i causes more bounded structure. This effect provides a negative energy for the structure which will produce smaller R_{max} and R_{vir} as well as earlier virialization time to the structure.

In the next section we will study the effect of cooling of baryonic matter at the final stage of virialization on structure formation.

4 Cooling Mechanism

Once the baryonic structure reaches to the virial condition, radial velocity of the structure converts to the dispersion velocity or in another word the baryonic gas thermalizes. The temperature of structure, using the kinetic energy of baryonic particles can rise up to $10^7 K$ and from the Saha equation we will have an ionized medium. The ionized plasma then cools down and the result is more contraction of the baryonic structure. On the other hand through the cooling, the baryonic structure can fragment into the small parts to generate stellar systems. During the cooling of baryonic matter, it will lose its kinetic energy and hence falls into the gravitational potential well and subsequently gains the kinetic energy (26). This cooling and heating continues until the system reaches to a quasi-steady state.

A simple parameter that represents the cooling of a gas is the ratio of cooling to the free fall time scale, $\tau = t_{cool}/t_{grav}$. The cooling time is defined by $t_{cool} = E/\dot{E} \approx 3\rho k_B T/2\mu\Lambda(T)$ and the dynamical time also results from the time scale for the free fall of a structure and is given by $t_{dyn} = \frac{\pi}{2}(2GMR^{-3})^{-1/2}$. If $\tau > 1$ then the gas can cool; but as it cools the gas can retain the pressure support by adjusting its pressure distribution. If $\tau < 1$ the gas will cool rapidly to a minimum temperature. This will lead to the loss of pressure support and the gas will undergo an almost free-fall collapse. In this case fragmentation into stellar units can occur. There are various physical processes contribute in cooling, depending on the temperature of the plasma. We assume cooling is dominated by plasma Bremsstrahlung radiation and recombination. At temperature larger than $10^7 K$, Bremsstrahlung dominates the cooling whereas in the range of $10^4 \sim 10^6$, recombination of gas is the main source of cooling. The net cooling rate is

$$C = \frac{dE}{dt dV} = n_e n_p \Lambda(T), \quad (23)$$

where $\Lambda(T)$ is the radiative cooling function and is expressed as

$$\Lambda(T) = (A_B T^{\frac{1}{2}} + A_R T^{\frac{-1}{2}}) \rho^2 \quad \frac{erg}{cm^3 s}. \quad (24)$$

$A_B \propto e^6/m_e^{3/2}$ represents cooling due to the bremsstrahlung and $A_R \simeq e^4 m_p A_B$ arises from the recombination. This expression is valid for temperatures above $10^4 K$. For lower temperatures, the cooling rate drops drastically because H

can no longer be significantly ionized by collisions. The radiative cooling function for temperatures above 10^7 is well approximated by

$$\Lambda(T) = 2.5 \times 10^{-27} T^{\frac{1}{2}} \frac{erg}{cm^3 s}. \quad (25)$$

Here we study the cooling condition of baryonic part of structure after the thermalization which $\tau = t_{cool}/t_{dyn} \ll 1$ is hold and we have almost free fall condition for the structure. Fig. (9) shows the variation of τ in terms of redshift for a galaxy mass structure, starting from the thermalization time to the quasi steady state. The duration of cooling for this structure in the Λ CDM model is about $\Delta z \simeq 0.07$. Fig. (10) shows the evolution of the size of structure in terms of redshift for this period. After thermalization structure freely falls until it reaches to a quasi steady state. Fig. (11) also indicates the evolution of the density contrast including the cooling effect after thermalization time.

To see the effect of variable dark energy on cooling time, we take a small structure with the mass of $10^6 M_\odot$. This mass is suitable for studying the evolution of the globular clusters and corresponds to the baryonic Jeans mass after the decoupling (27). According to the structure formation scenario we expect that this structure has a dark matter component. However the observations of dispersion velocity show that these structures almost have no dark matter. The pre-galactic model for the globular cluster and tidal striping of dark halo by Galaxy can explain the lack of dark matter in these structures (28). It should be noted that in the formation of these structures we don't consider merging effect as naturally is taken account in the N-body simulations.

Variable dark energy causes the structure thermalizes and cools at the higher redshifts (see table 2). For instance, taking the parameters $w_0 = -1.45$ and $b = 1.35$, structures with globular cluster mass thermalize at $z \sim 2.17$ and stop cooling at $z \sim 1.94$. For a larger structure with a galaxy mass of $10^{11} M_\odot$, the corresponding thermalization redshift occurs at $z \sim 0.7$ (see Fig. 7). Comparing with the globular cluster we can conclude that the first star bursts would happened in the globular clusters. The high metalicity with the low rotation of globular cluster in the galactic halo supports this hypothesis.

5 Conclusion

In this work we extend simple top-hat model into two component dark matter-baryonic structure. The initial condition for the sub-horizon size structures is taken at the last scattering surface. The scale of $\lambda < d_H$ for the structures guarantees applying approximately the Newtonian mechanics. Using the Harrison-Zeldovich spectrum for the perturbations of dark matter, we obtained

the evolution of each component of the structure.

For the dark matter part, we showed that density contrast in the small mass structures grows faster than the larger ones and subsequently reaches to the maximum radius and virializes at the higher redshifts. This behavior of structures implies that the star burst should take place at the smaller structures as dwarf galaxy and globular clusters. An observable parameter of structures to compare with the model is the power spectrum. We calculated the mass variance of structures in various scales at the present time and compared $\sigma_8 \sim 0.8$ from the model with that of observation from the weak lensing. For studying the dynamical effect of background on the evolution of the structures, we applied a logarithmic variable dark energy model and showed that the structures in this model evolve faster than that of Λ CDM.

References

- [1] G. F. Smoot *et al.*, ApJ **396**, 1 (1992)
- [2] G. Hinshaw *et al.*, ApJS **170**, 263 (2007).
- [3] D. N. Spergel *et al.*, ApJS **148**, 175 (2003).
- [4] D. N. Spergel *et al.*, ApJS **170**, 377 (2007).
- [5] V. Springel *et al.*, 2005, Nature, 435, 629.
- [6] P. J. E. Peebles 1980, The Large-Scale Structure of the Universe (Princeton University Press, Princeton, New Jersey).
- [7] J. Silk, ApJ **151**, 459 (1968)
- [8] R. Mansouri and S. Rahvar, IJMPD **11**, 321 (2002).
- [9] S. Rahvar, IJMPD **12**, 79 (2003).
- [10] T. Padmanabhan, 1993, Structure Formation in the Universe, Cambridge Univ. Press.
- [11] T. Padmanabhan, 2002, Theoretical Astrophysics, Vol III. Cambridge Univ. Press.
- [12] E. R. Harrison, Phys. Rev. D **1**, 2726 (1970)
- [13] Y. Zeldovich, Astr. Astron. **5**, 8 (1970)
- [14] J. A. Peacock, 1999, Cosmological Physics. Cambridge Univ. Press
- [15] T. Hamana, ApJ **597**, 98 (2003)
- [16] A. G. Riess *et al.*, ApJ **607**, 665 (2004)
- [17] O. Lahav, P. B. Lilje, J. R. Primack, M. J. Rees, MNRAS. **251**, 128 (1991).
- [18] L. M. Wang, P. J. Steinhardt, ApJ. **508**, 483 (1998).
- [19] I. T. Iliev, P. R. Shapiro, MNRAS. **325**, 468 (2001).
- [20] N. N. Weinberg, M. Kamionkowski, MNRAS. **341**, 251 (2003).
- [21] R. A. Battye, J. Weller, Phys. Rev. D **68**, 083506 (2003).
- [22] D. F. Zeng, Y. H. Gao, arXiv:astro-ph/0412628.
- [23] D. F. Mota, C. van de Bruck, Astron. Astrophys. **421**, 71 (2004).

- [24] C. Wetterich, Phys. Lett. B **594**,17 (2004)
- [25] M. S. Movahed, S. Rahvar, Phys. Rev. D **73**, 083518 (2006)
- [26] P. E. J. Nulsen, A. C. Fabian, MNRAS **271**, 561 (1995)
- [27] P. J. E. Peebles and Dicke, R. H., ApJ **154**, 891 (1968)
- [28] E. I. Rosenblatt., S. M. Faber, and G. R. Blumenthal, ApJ **330**, 191 (1998).
- [29] S. Basilakos, N. Voglis, MNRAS, **374**, 269 (2007).

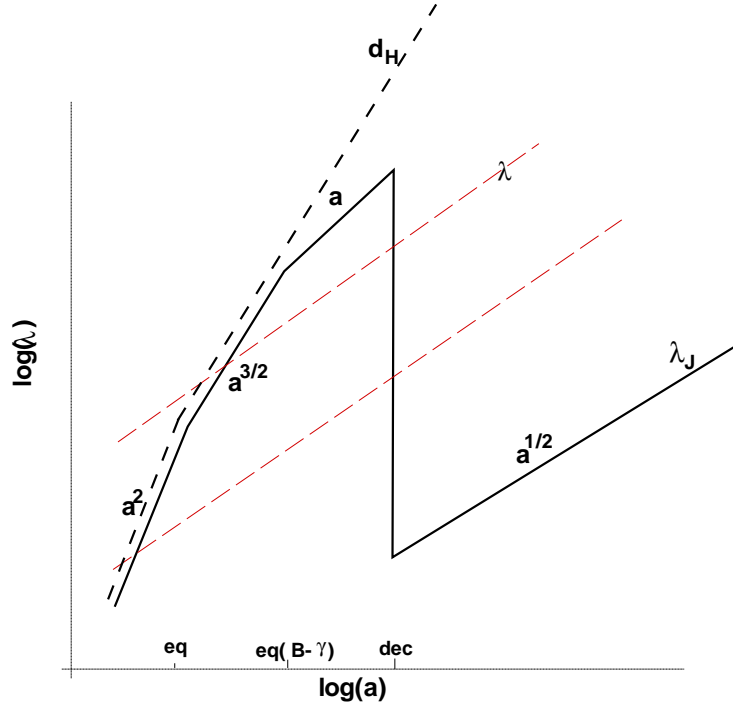


Fig. 1. Size of horizon of universe (short dashed line), size of structure (long dashed line) and Jeans length (solid line) of baryonic structures in terms of scale factor in logarithmic scale. At the last scattering surface the Jeans mass of baryonic matter decreases and baryonic structure with sub-horizon scale can grow after this epoch.

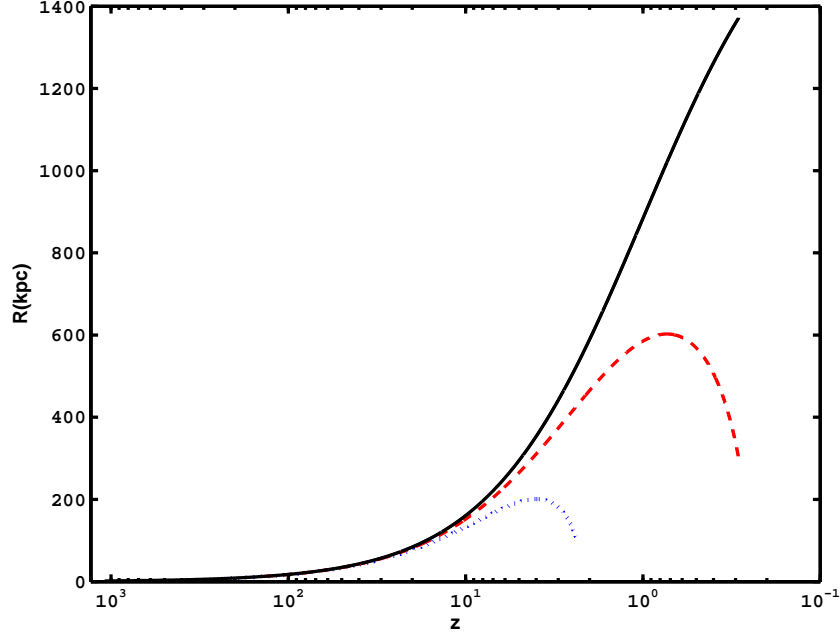


Fig. 2. Dependence of radii of halo (dotted-line) and baryonic (dashed-line) components for a structure with a galaxy mass in top-hat model in terms of redshift, compared with that of background (solid-line). Background is taken Λ CDM model with the corresponding parameters of $\Omega_m^{(0)} = 0.3$, $\Omega_\Lambda^{(0)} = 0.7$ and $H_0 \sim 70 \text{ Km/sMpc}^{-1}$.

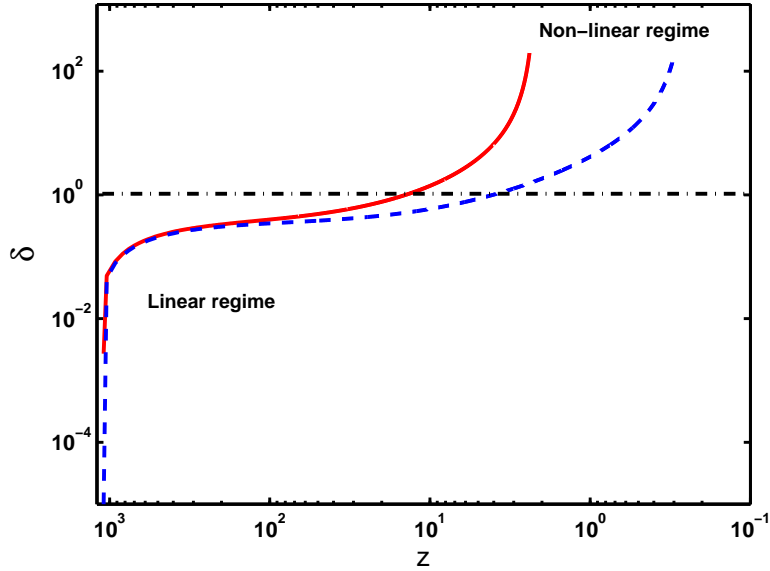


Fig. 3. Density contrast evolution of baryonic (dashed-line) and dark matter (solid-line) in terms of redshift. The horizon line represents $\delta = 1$, separate the linear and non-linear regimes.

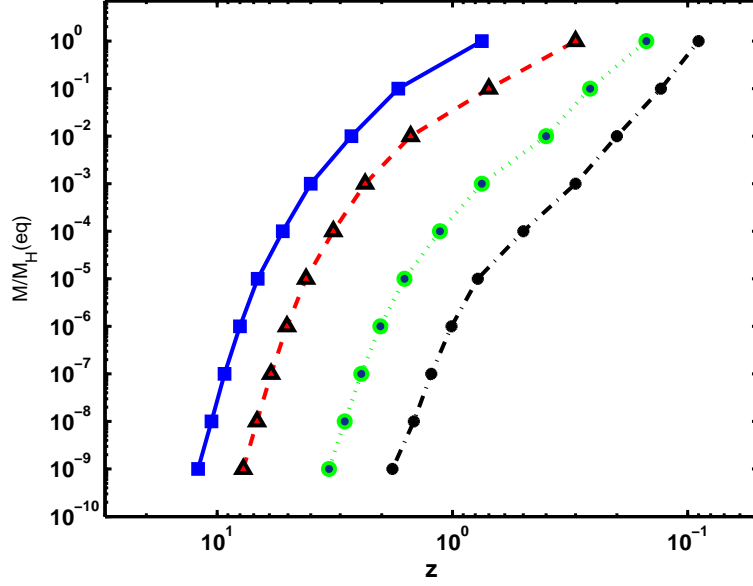


Fig. 4. Dependence of Mass (normalized to M_H) to the characteristic redshifts of the structures. Solid line represents redshift corresponds to the maximum radius of a structure in terms of mass. Dashed line represents the dependence of virialization redshift to the mass of dark matter structure. Dotted and dashed-dotted lines represent the maximum radius and virialized redshifts for the baryonic component of the structure, respectively.

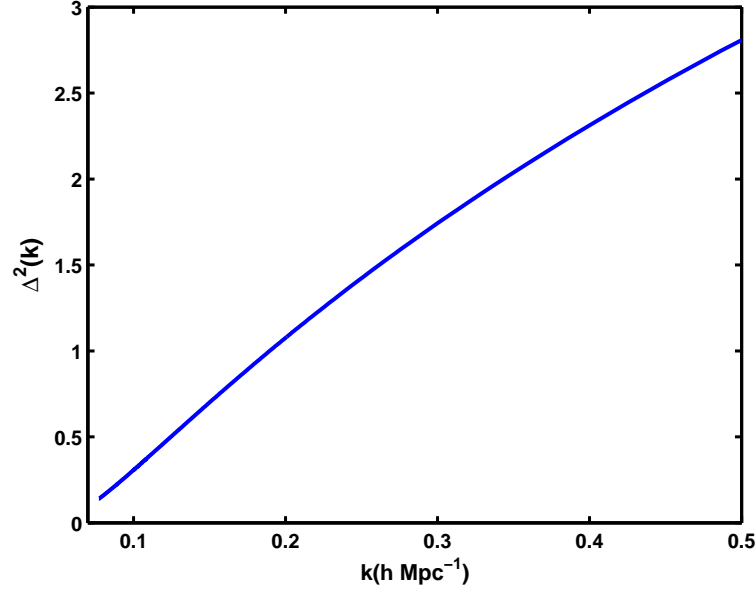


Fig. 5. The power spectrum calculated by the two component top-hat model is derived in terms of k .

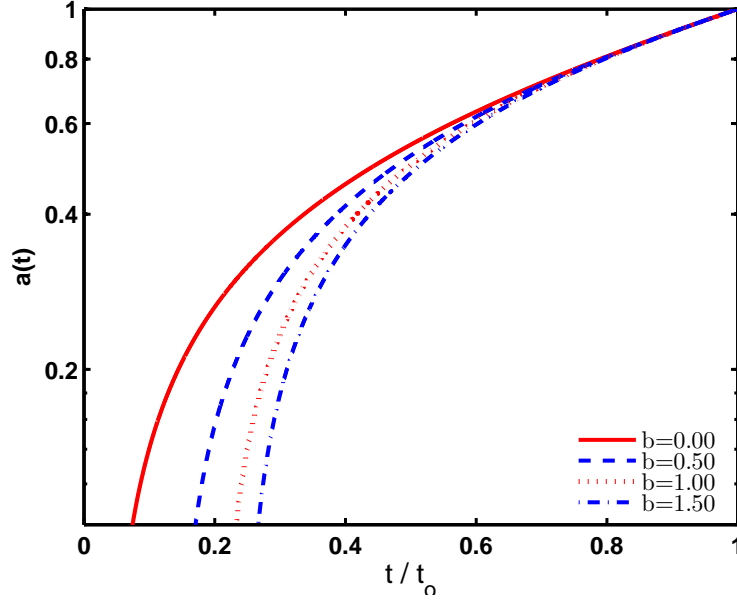


Fig. 6. Dynamics of scale factor in terms of cosmic time (normalized to t_0) with a variable dark energy model given by Eq. (20). Solid line stands for $b = 0$ (Λ CDM), dashed line $b = 0.5$, dotted line $b = 1.0$ and dashed-dotted line $b = 1.5$.

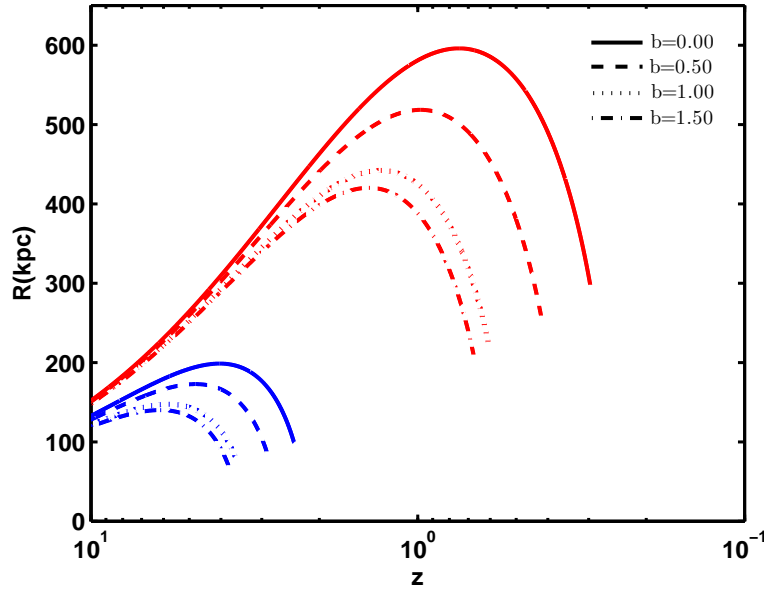


Fig. 7. The effect of bending parameter in logarithmic variable dark energy model on the dynamics of structure in terms of redshift. Red lines represent the baryonic component and blue lines stand for the dark matter component. The bending parameters are chosen as $b = 0$ (solid line), $b = 0.5$ (dashed line), $b = 1$ (dotted line) and $b = 1.5$ (dashed-dotted line). The equation of state is fixed with $\omega_0 = -1.45$.

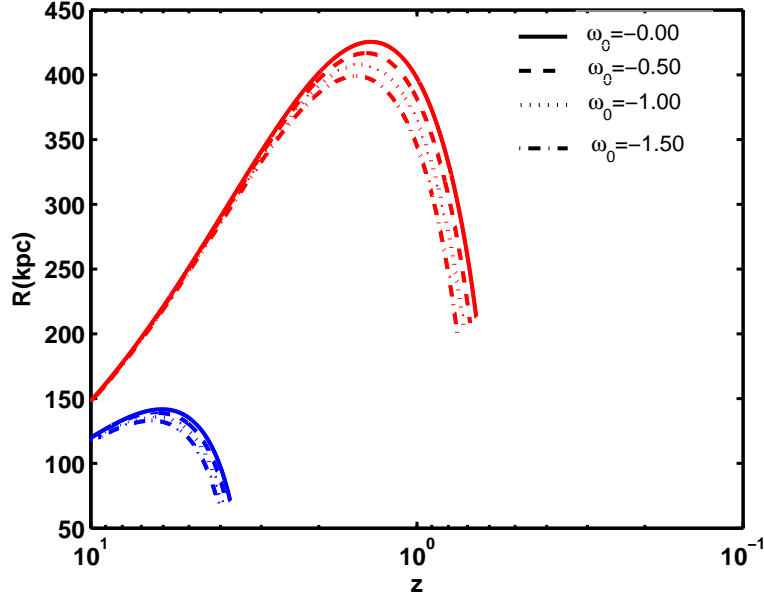


Fig. 8. The effect of equation of state in logarithmic variable dark energy model on the dynamics of structure in terms of redshift. Red lines represent the baryonic component and blue lines stand for the dark matter component. The equation of states are chosen as $w_0 = 0$ (solid line), $w_0 = -0.5$ (dashed line), $w_0 = -1$ (dotted line) and $w_0 = -1.5$ (dashed-dotted line). The bending parameter is fixed with $b = 1.35$.

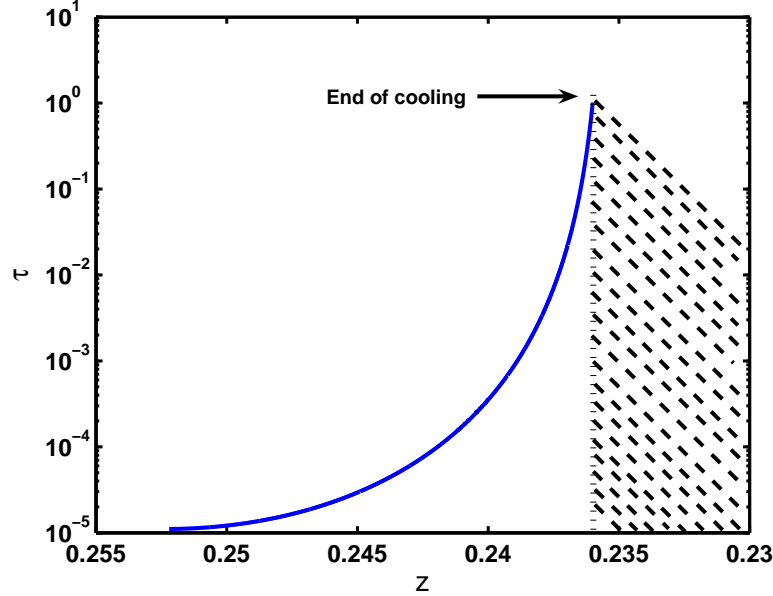


Fig. 9. Variation of τ in term of redshift for a galaxy mass structure. τ is plotted from thermalization till the quasi-steady state phase of baryonic structure. Dashed era represents the stable zone for the structure where the cooling is negligible.

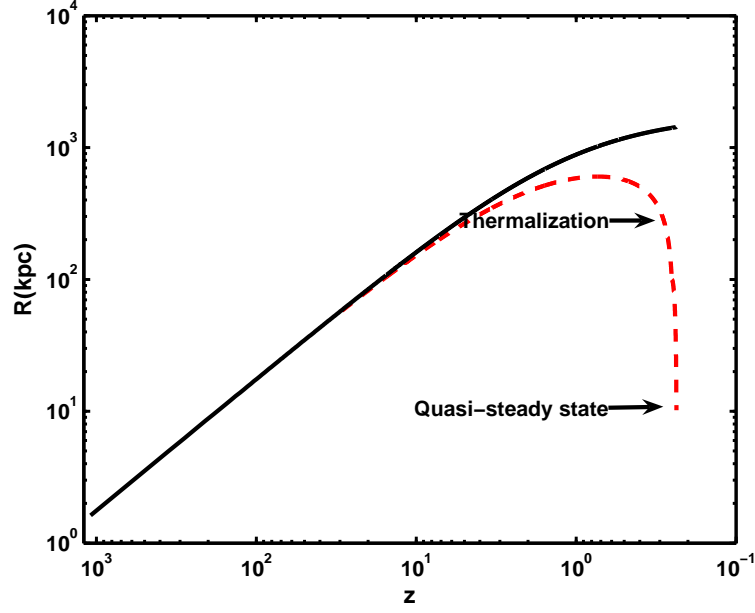


Fig. 10. Dynamics of radius of galaxy mass structure in terms of redshift (dashed line). After thermalization we will have free fall collapse of structure until quasi steady state time. Solid line represents the dynamics of background for comparison.

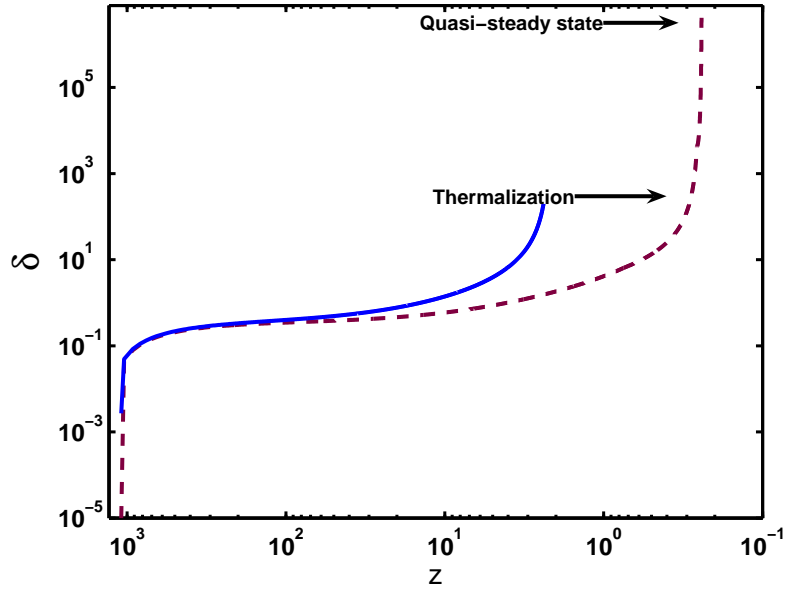


Fig. 11. Evolution of density contrast in terms of redshift for baryonic (dashed line) and dark matter (solid line) components of a galaxy mass structure. After thermalization we will have almost four order of magnitude increase of the baryonic density contrast.

Table 1

Numerical results from the evolution of structures with various masses. First column shows the range of mass of structures and subscript in M represents mass in $10^n M_\odot$. Second column is the corresponding redshift to entering to the Horizon. The density contrast of dark matter at the decoupling epoch is in third column. Forth and Fifth columns are the corresponding redshift of maximum radius for the dark matter and virialization of the dark structure. Sixth and seventh columns are the same as the forth and fifth columns for the baryonic structure.

M	z_{enter}	δ_{dec}^d	z_m^d	z_{vir}^d	z_m^b	z_{vir}^b
M_{15}	5.90×10^3	1.9×10^{-4}	0.70	0.30	0.15	0.10
M_{14}	1.27×10^4	1.2×10^{-3}	1.70	0.70	0.26	0.15
M_{13}	2.74×10^4	2.0×10^{-3}	2.60	1.50	0.40	0.20
M_{12}	5.90×10^4	2.7×10^{-3}	4.00	2.30	0.75	0.30
M_{11}	1.27×10^5	3.4×10^{-3}	5.20	3.20	1.13	0.50
M_{10}	2.74×10^5	4.2×10^{-3}	6.70	4.20	1.60	0.78
M_9	5.90×10^5	4.9×10^{-3}	8.00	5.00	2.00	1.00
M_8	1.27×10^6	5.6×10^{-3}	9.30	5.90	2.40	1.20
M_7	2.74×10^6	6.3×10^{-3}	10.50	6.70	2.80	1.40
M_6	5.90×10^6	7.1×10^{-3}	12.00	7.75	3.30	1.80

Table 2

The effect of bending parameter on duration of cooling of baryonic structure in logarithmic variable dark energy model. Mass of structure is taken $10^6 M_\odot$. At the first column we fixed ($w_0 = -1.45$) and the second column shows the duration of cooling for various bending parameters. In the third column we fixed bending parameter ($b = 1.35$) while the equation of state w_0 has different values with corresponding duration of redshift is indicated in the fourth column.

$\omega_0 = -1.45$	$z_{starburst}$	$b = 1.35$	$z_{starburst}$
$b = 0.00$	[1.82, 1.65]	$\omega_0 = 0.00$	[1.80, 1.62]
$b = 0.50$	[2.15, 1.84]	$\omega_0 = -0.50$	[2.04, 1.80]
$b = 1.00$	[2.22, 1.98]	$\omega_0 = -1.00$	[2.12, 1.90]
$b = 1.50$	[2.25, 2.00]	$\omega_0 = -1.50$	[2.19, 1.95]